Estimation of heat, water, and black carbon fluxes during the fire induced by the Hiroshima A-bomb

Michio Aoyama[a], Noriyuki Kawano[b], Toshio Koizumi[c] , Takao Okada[d], Yoshihiro Okada[e], Megu Ohtaki[f] and Takahiro Tanikawa[c]

[a] *Geochemical Research Department, Meteorological Research Institute, Nagamine 1-1, Tsukuba, Ibaraki 305-0052, Japan*
[b] *Institute for Peace Science, Hiroshima University, Higashisenda-machi 1-1-89, Naka-ku, Hiroshima 730-0053, Japan* [c] *Architecture and Civil Engineering, Chiba Institute of Technology, Tsudanuma 2-17-1, Narashino, Chiba 275-0016, Japan*
[d] *c/o Research Division, Atomic Bomb Survivors Relief Department Health and Welfare Bureau, Hiroshima City Hall, Kokutaiji-machi 1-6-34, Naka-ku, Hiroshima 730-8586, Japan*
[e] *Heiwa-Kensetu Co. Ltd., Kawaguchi-cyou 1-16-35, Fukuyana, Hiroshima 720-0822, Japan*
[f] *Department of Environmetrics and Biometrics, Research Institute for Radiation Biology and Medicine, Hiroshima University, Kasumi 1-2-3, Minami-Ku, Hiroshima 734-8551, Japan*

Abstract

The amount of flammable materials in traditional Japanese houses in the Hiroshima region in July 1945 was estimated in terms of kg m^{-2} in each 50 m grid in 8 km x 8 km region. Then, the amount of flammable materials was converted to heat, water, and black carbon fluxes based on the duration of the fire induced by the A-bomb as a function of time and space. The average heat flux in the region was 14.4 kJ s^{-1} m^{-2}, and it ranged from 0.5 to 96.5 kJ s^{-1} m^{-2}. The total heat released during the fire was 7 PJ. In total, 0.22 Tg of water was produced and released during the fire. The total amount of black carbon produced and released during the fire was 0.02 Tg, when we assume that 10% of the fuel was under reducing conditions. The time-dependent fluxes of heat, water, and carbon were also calculated in each 50 m grid.

1. Introduction

To conduct numerical model simulation of distribution of radioactive fallout and black rain after the explosion of the Hiroshima A-bomb in 6 August 1945, initial conditions and boundary conditions such as distribution of fission products in the mushroom cloud, heat, water and carbon fluxes from surface of the ground should be given by appropriate grid size and time scale. HiSoF members studied to create database for this purpose and combined them as a database. So-called ‘Black Rain’, which might include radioactivity, fell around the western part of Hiroshima City and the northwest suburbs for several hours just after the explosion of the atomic bomb on August 6, 1945. In those days, there was only one official weather station in the neighborhood of Hiroshima City, the Eba meteorological observatory, which was located 3.7 km southwest from the hypocenter. Therefore, questionnaire surveies had been used to grasp

ISBN 978-4-9905935-0-6
Revisit the Hiroshima A-bomb with Database: 43-54

the actual situation of spatial-time distribution of 'Black Rain' (Uda et al., 1947, Uda et al., 1953, Masuda, 1989, Otaki, 2011). Recently, Hiroshima City carried out a questionnaire survey of about 37,000 inhabitants of Hiroshima and its suburbs who might have experienced 'Black Rain', investigating the start time, end time, and location of the rain. Based on the recent questionnaire, Otaki concluded that the estimated rainy area is about five to six times wider than Uda's 'heavy rain area' (Otaki, 2011). From a view point of radioecological effect of radioactive fallout originated from the A-bomb, the details of radioactive contamination by black rain are important but it is not yet clear.

On the other hand, numerical model simulation of fallout using a preliminary chemical transport model was conducted in 1990 to evaluate radioactive fallout from Hiroshima A-bomb and it was concluded that the fallout area of Hiroshima A-bomb was similar with that of Uda's heavy rain area (Yoshikawa, 1990).

It already passed two decades from the firtst numerical model simulation of fallout of the Hiroshima A-bomb in 1990, it might possible to conduct improved numerical model simulations using latest chemical transport models and high performance super computers. If so, heat flux and water flux during the induced urban fire by the Hiroshima A-bomb are important to simulate the clouds and precipitation due to the Hiroshima A-bomb. Therefore, we estimate amount of flamable materials in traditional Japanese houses in Hiroshima region in 1940s are estimated in terms of kg m^{-2} in each 50 meters grid. Then, amount of the flamable materilas was converted to heat, water, carbon dioxide, and black carbon fluxes based on the duration of induced fire as function of time and space. These heat, water, carbon dioxide, and black carbon fluxes would be used as boundary conditions for the chemical transport models together with meteorological field given by another research (Chiba, 2011)

2. Basics of heat, water, carbon dioxide, and black carbon flux estimation

The main products of the combustion of wood are carbon dioxide, water, and heat, which are produced when the cellulose in wood reacts with oxygen in the air, as shown in equation (1):

$$C_6H_{12}O_6 + 6O_2 = 6CO_2 + 6H_2O \quad (1)$$

When cellulose burns under oxygen-rich conditions, one part oxygen is consumed for each part cellulose, producing one part carbon dioxide and one part water. Thus 1 kg of cellulose can produce 1.47 kg of carbon dioxide and 0.60 kg of water.

The complete combustion of cellulose produces neither ash nor smoke. However, oxygen-deficient conditions will produce one part carbon and one part water as products, as shown in equation (2):

$$C_6H_{12}O_6 = 6C + 6H_2O \quad (2)$$

Wood also contains small amounts of nonflammable minerals that are left behind as ash. In this study, ash is ignored because the portion of ash was likely to be very small (need ref. here). Therefore, we assume that the combustion of wood produces carbon or carbon dioxide, depending on whether the conditions are oxidizing (oxygen rich) or reducing (oxygen deficient), and water independent of the conditions.

There are two major chemical components in wood: lignin (18–35%) and carbohydrate (65–

75%). Both are complex, polymeric materials. Minor amounts of extraneous materials, mostly in the form of organic extractives and inorganic minerals (ash), are also present in wood (usually 4–10%). Overall, wood has an elemental composition of about 50% carbon, 6% hydrogen, 44% oxygen, and trace amounts of several metal ions (Pettersen, 1984). The carbohydrate portion of wood comprises cellulose and the hemicelluloses. Cellulose content ranges from 40% to 50% of the dry weight of wood, and hemicellulose content ranges from 25% to 35%. The atomic ratio of carbon, hydrogen, and oxygen in whole wood is $C_8H_{12}O_5$, which is slightly different from that of cellulose, $C_6H_{12}O_6$. The mass of products from 1 kg of cellulose and wood combustion in both oxygen-deficient condition and oxygen-rich conditions are shown in Table 1.

Table 1. Mass of combustion products from 1 kg of cellulose and wood.

Product	Cellulose (kg)	Wood (kg)
Black carbon	0.40	0.51
Carbon dioxide	1.47	1.53
Water	0.60	0.57

As shown in Table 1, the mass of products from 1 kg of wood combustion in complete oxygen-deficient condition are 0.51 kg of black carbon and 0.57 kg of water, respectively. When we assume oxygen rich condition, the mass of products from 1 kg of wood combustion in complete oxygen-deficient condition are 1.53 kg of carbon dioxide and 0.57 kg of water, respectively. The oxygen conditions for the fire induced by the A-bomb on 6 August 1945 are unknown, so we assume that 10 % of wood was at under reducing conditions. This assumption would result in 0.05 kg of black carbon, 1.48 kg of carbon dioxide, and 0.57 kg of water being produced and released per 1 kg of wood combustion. The weight ratio between black carbon and water is about 9 % when we assume that 10 % of wood was at under reducting conditions which might be similar with a weight ratio between black carbon and water in the black rain observed in 1945. In fact, reproduced black rains of which black carbon concentrations ranged from 5 % to 70% are presented as unknown samples to the A-bomb survivors and they chose the samples ranged from 5 % to 15 % are close to the black rain in 1945. Therefore, we are safe to say that 10 % of wood might be at under reducting conditions.

3. Method

3.1 Study domain and grid size

We set 8 km (east–west, x) × 8 km (north–south, y) as interested domain for the calculation of heat, water, carbon dioxide and black carbon fluxes. A center of this domain is the hypocenter of the A-bomb. Figure 1 illustrates the center region of the interested domain, which covers 4 km (east–west, x) × 4 km (north–south, y).

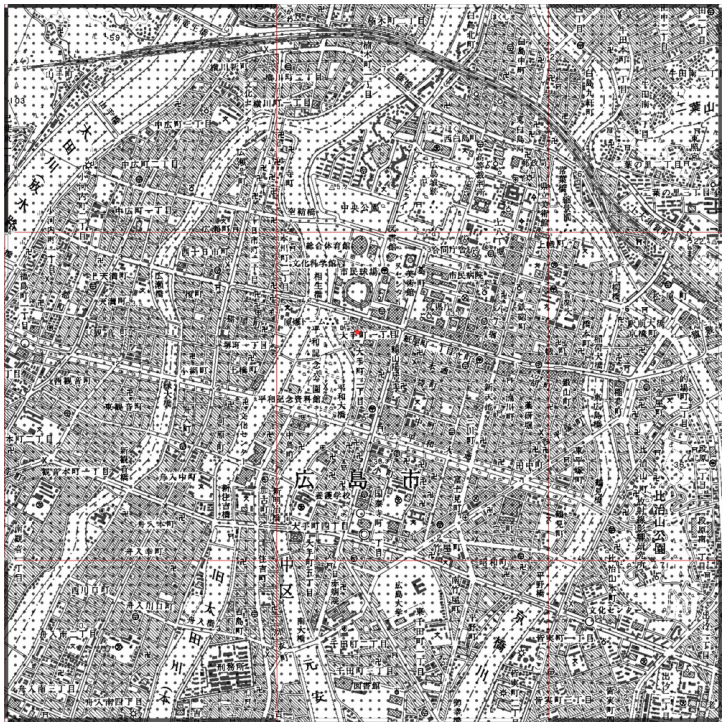

Figure 1 The center of computational domain which covers 4 km (east-west, X) × 4 km (north-south, Y). The grid size is 50 meters in both X- and Y- axises.

3.2 Amount of flammable materials

Figure 2 shows a map of houses and buildings in the Hiroshima area before the A-bomb exploded on 6 August 1945, and Figure 3 shows the distribution of destroyed houses and buildings in the area after the A-bomb exploded.

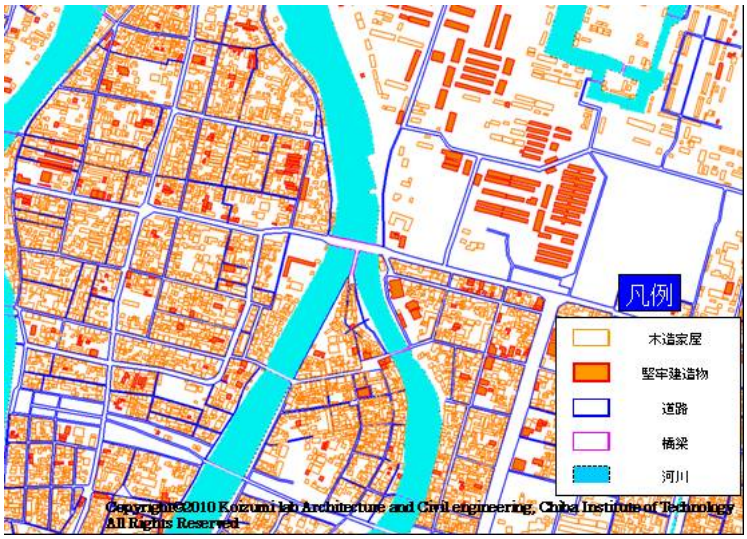

Figure 2 A map of buildings/houses of center of Hiroshima City near hypocenter for 25 July 1945, just before A-bomb on 6 August 1945, based on aerial photographs taken by US army.

Orange frame: Japanese traditional wooden houses.

Filled by red within orange frame: Buildings.

Dark blue: Roads. Purple: Bridges. Blue: Rivers.

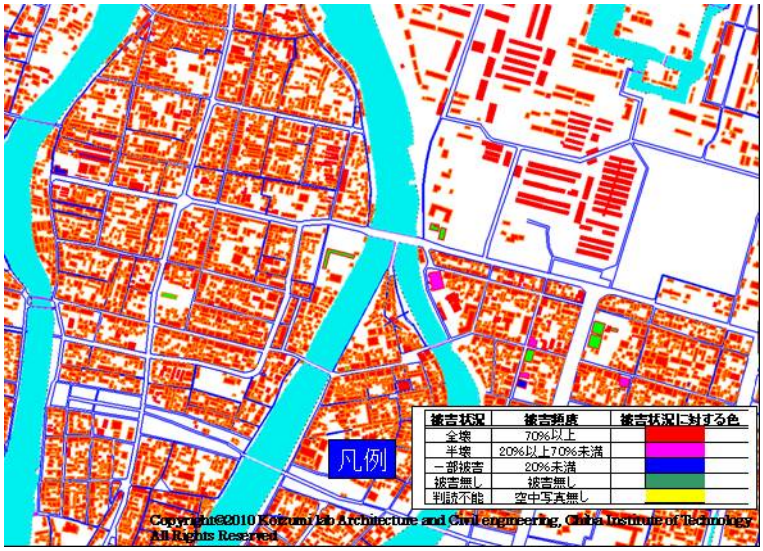

Fugure 3 A disaster map of buildings/houses of center of Hiroshima City near hypocenter for 8 August 1945, just after A-bomb on 6 August 1945, based on aerial photographs taken by US army.

Marked red: Destroyed/burned more than 70 %.

Marked pink: Destroyed/burned between 20 % and 70 %.

Marked dark blue: Destroyed/burned less than 20 %.

Marked green: Not damaged.

Marked yellow: No photograph available, then not judged.

Purple: Bridges.

Blue: Rivers.

The total number of Japanese traditional houses destroyed by the A-bomb and resulting fire was estimated to be 34,839, whereas 1918 buildings were destroyed. The estimated number of houses is smaller than 67,860 which was reported by the local government in 1971 (Hiroshima City, 1971) because the method to count houses based on photographs used in this study (Koizumi; 2011, this volume) could not distinguish connecting houses.

Table 2. Number of Japanese houses destroyed by fire on 6 August 1945

Type	Total
One-story house	23,368
Two-story house	9233
School, inn, or temple	2238
Total	34,839

We estimated the total mass of flammable materials in each 50-m grid using a database of destroyed houses based on aerial photographs taken by the U.S. Army, as described by Koizumi (this volume), and results of field research of flammable materials in Japanese traditional houses per unit area (Okada and Aoyama; 2011, this volume). The area and height of each resolved house were categorized into three classes: one-story house, two-story house, and large wooden building. Then using the reference density for each class and area, we calculated the mass of flammable materials in each house. The latitude and longitude at the center of each house was

converted to distance from the hypocenter, and these were assigned a corresponding grid number. Finnaly, we integrated the mass of flammable materials, *M* kg, in each 50-m grid.

3.3 Heat flux estimation

Considering that the total mass of flammable materials in each 50-m grid = *M* kg, the calorific value of flammable materials in each 50-m grid was calculated using the heat yield of combustion of pine, 17.9 MJ kg^{-1} (DiNenno et al., 1995a), such that the calorific value of flammable materials in each 50-m grid = *M* kg × 17.9 MJ kg^{-1}. Given that the total area of each 50-m grid = 2500 m^2, and the average burning period = 8 h or 28800 s (Kawano et al., this volume), the average heat release rate per unit area per second = (*M* × 17.9)/(2500 × 28800) MJ s^{-1} m^{-2}.

Uncertainty of heat flux estimation mainly depends on the mass of flammable materials in each 50-m grid, conversion factor from mass to heat, condition of combustion, type of wood. For the mass of flammable materials in each 50-m grid, we use only three types, one-story, two-story and school et al., therefore this would cause 20-30 % uncertainty on the estimation of the mass of flammable materials in each 50-m grid. Conversion factors also varied 10-20% depend on type of wood and literature. It is difficult to estimate uncertainty caused by condition of combustion, we adopt 10 ± 5 % as a range of reducting condition as discussed in chapter 2. Summing up these uncertainty, about 35% is given as an overall uncertainty for our heat flux estimation.

3.4 Water, carbon dioxide and black carbon fluxes

As already discussed above, water, carbon dioxide and black carbon fluxes can be given below.

The average water flux per unit area per second

$$=(M \text{ x } 0.57)(2500\text{x}28800) \text{ kg s}^{-1} \text{ m}^{-2}.$$

The average carbon dioxide flux per unit area per second

$$= (M \text{ x } 1.48)(2500\text{x}28800) \text{ kg s}^{-1} \text{ m}^{-2}.$$

The average black carbon flux per unit area per second

$$= (M \text{ x } 0.05)(2500\text{x}28800) \text{ kg s}^{-1} \text{ m}^{-2}.$$

Where *M* is the total mass of flammable materials in each 50-m grid.

4. Results and discussion

4.1 Heat flux

In Figures 4 and 5, distributions of average heat flux (MJ s^{-1} m^{-2}) in each 50-m grid within the 4 km × 4 km and 8 km × 8 km are shown, respectively. A part of the destroyed area located southwest of the hypocenter could not be analyzed because clouds covered the area when the aerial photographs were taken. Although the average heat flux in the region was 14.4 kJ s^{-1} m^{-2}, it ranged from 0.5 to 96.5 kJ s^{-1} m^{-2} as shown in the Figures 4 and 5. When we look at within 1

km × 1 km region from the hypocenter, the averaged heat flux at north-west region is relatively high rather than those in north-east, shouth-west and south-east regions.

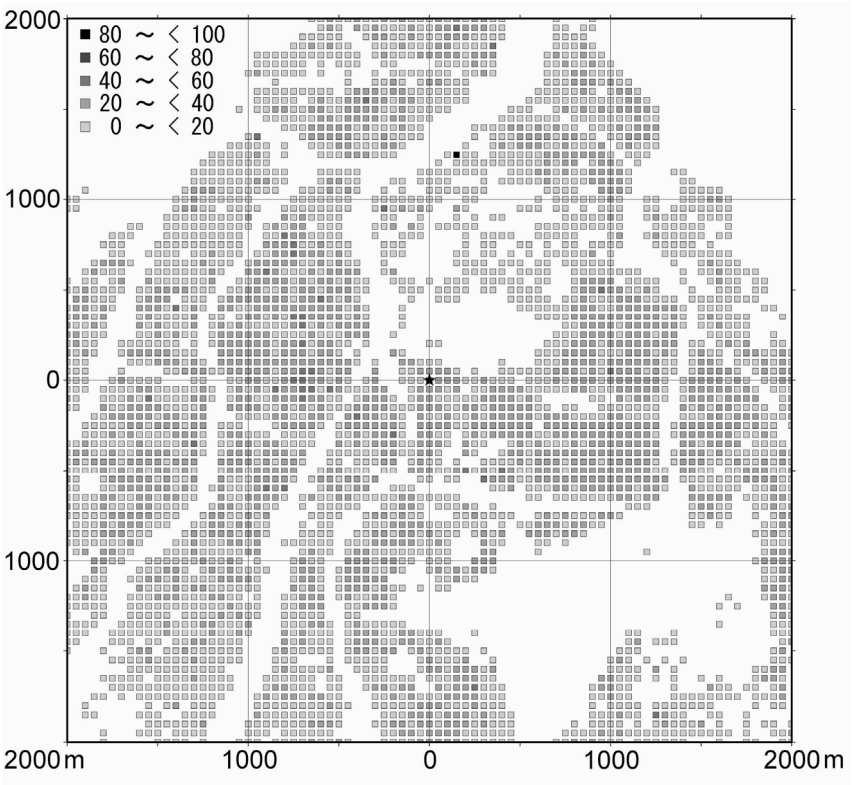

Figure 4 Distribution of average heat flux in each 50 m grid within 4 km × 4km area of hypocenter of the A-bomb as a same area as shown in figure 1. A star marked at a location (0 m, 0 m) is the hypocenter of A-bomb. Unit: MJ s^{-1} m^{-2}

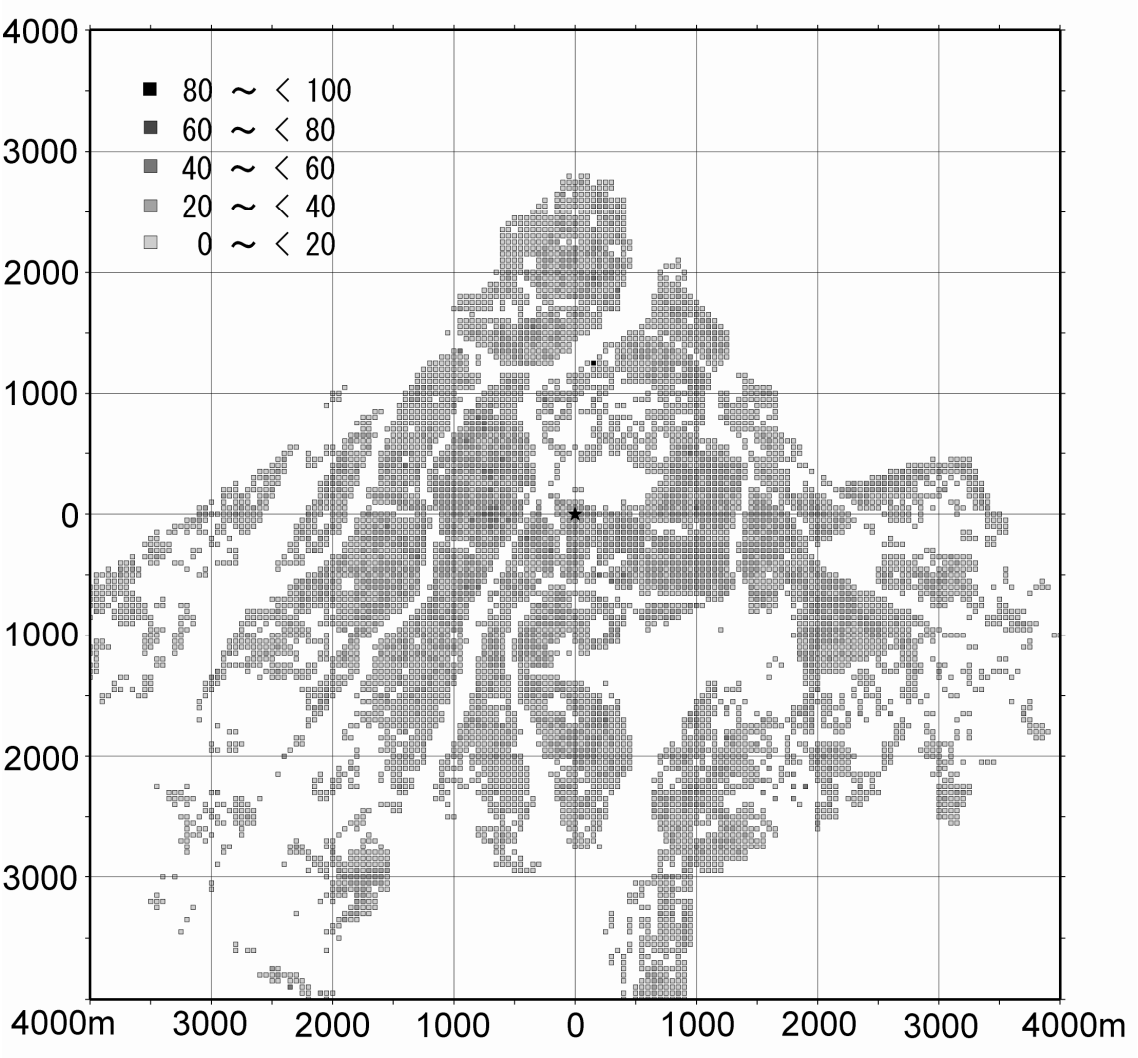

Figure 5 Distribution of average heat flux in each 50 m grid within 8 km x 8 km area of hypocenter of the A-bomb. A star marked at a location (0 m, 0 m) is the hypocenter of A-bomb. Unit: MJ s^{-1} m^{-2}

We estimated the total mass of flammable materials to be 0.39×10^9 kg, such that the total heat released during the fire induced by the A-bomb was estimated to be 7.02×10^{15} J (see Table 3 for representative values from nine grids). A part of the destroyed area located southwest of the hypocenter could not be analyzed because clouds covered the area when the aerial photographs were taken. Therefore, our estimation of total mass of flammable materials and some resulting values might be underestimated by a few percent. In the database, the average value of the mass of flammable materials in a 50-m grid will be inserted for the area lacking data.

Table 3. Examples of the total area of houses, coverage, total mass of flammable materials, total heat produced, heat produced per unit area, and average heat flux for nine 50-m grids around the hypocenter of the A-bomb.

Distance (m)	Direction (degree)	Area (m^2)	Coverage (%)	Total mass of flammable materials (10^3 kg)	Total heat produced (TJ)	Heat produced per unit area (MJ m^{-2})	Average heat flux (MJ s^{-1} m^{-2})
0	0	553	22	70	1.24	498	0.017
50	0	928	37	104	1.86	744	0.026
50	90	763	31	85	1.53	612	0.021
50	180	1192	48	96	1.72	688	0.024
50	270	601	24	47	0.84	335	0.012
71	45	988	40	82	1.47	587	0.020
71	135	1276	51	95	1.70	681	0.024
71	225	1029	41	120	2.15	858	0.030
71	315	1195	48	137	2.45	981	0.034

For the time-dependent heat flux, we assumed that the progress of combustion of houses follows a scenario as described by DiNenno et al. (1995b). In general, compartment fires are discussed in terms of the following stages: ignition, growth, flashover, fully developed fire, and decay. Because no fire control measures were undertaken due to the total destruction of fire control systems in Hiroshima after the A-bomb, we assumed the fire followed this scenario. We assumed that the growth period was about 3 h, based on the analysis by Kawano et al. (this volume), which shows good agreement with DiNenno et al. (1995b), when we consider a larger opening factor. A scenario of the rate of heat release is shown in Figure 6.

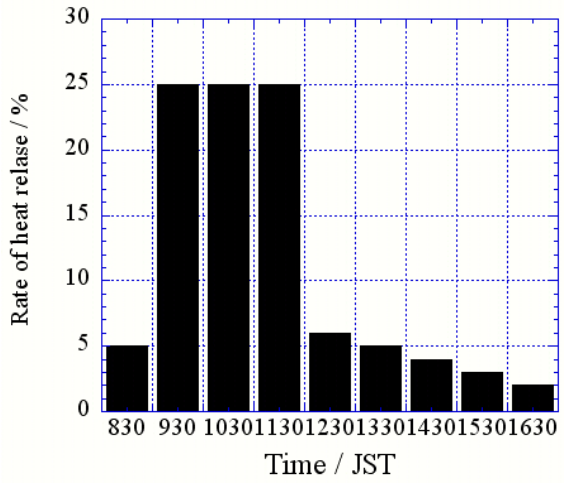

Figure 6 A scenario of a rate of heat release for the urban fire of which duration is 8 hours just after A-bomb explosion.

Therefore using total mass of flammable materials in each grid and the times that the fire began and ended in each grid, the time-dependent heat flux can be calculated, as shown in Table 4.

Table 4. Examples of time-dependent heat flux for nine 50-m grids around the hypocenter of the A-bomb. The bomb was dropped at 08:15 h.

Distance (m)	0	50	50	50	50	71	71	71	71
Direction (degree)	0	0	90	180	270	45	135	225	315
Time of day	Time-dependent heat flux (MJ s^{-1} m^{-2})								
08:30	0.028	0.041	0.034	0.038	0.019	0.033	0.038	0.048	0.054
09:30	0.035	0.052	0.043	0.048	0.023	0.041	0.047	0.060	0.068
10:30	0.035	0.052	0.043	0.048	0.023	0.041	0.047	0.060	0.068
11:30	0.035	0.052	0.043	0.048	0.023	0.041	0.047	0.060	0.068
12:30	0.008	0.012	0.010	0.011	0.006	0.010	0.011	0.014	0.016
13:30	0.007	0.010	0.009	0.010	0.005	0.008	0.009	0.012	0.014
14:30	0.006	0.008	0.007	0.008	0.004	0.007	0.008	0.010	0.011
15:30	0.004	0.006	0.005	0.006	0.003	0.005	0.006	0.007	0.008
16:30	0.003	0.004	0.003	0.004	0.002	0.003	0.004	0.005	0.005
Average	0.017	0.026	0.021	0.024	0.012	0.020	0.024	0.030	0.034

The heat produced by the fire would have been proportional to the oxygen condition, which is unknown. Given our assumption that 10% of the fuel was under reducing conditions, the total produced heat of 7.02×10^{15} J is decreased to 6.32×10^{15} J.

4.2 Water flux

An estimate of the water flux from the fire induced by the A-bomb was calculated based on the total mass of flammable materials in each grid and the production constant of water (Table 1). The distribution of averaged water flux for the region is shown in Figure 7.

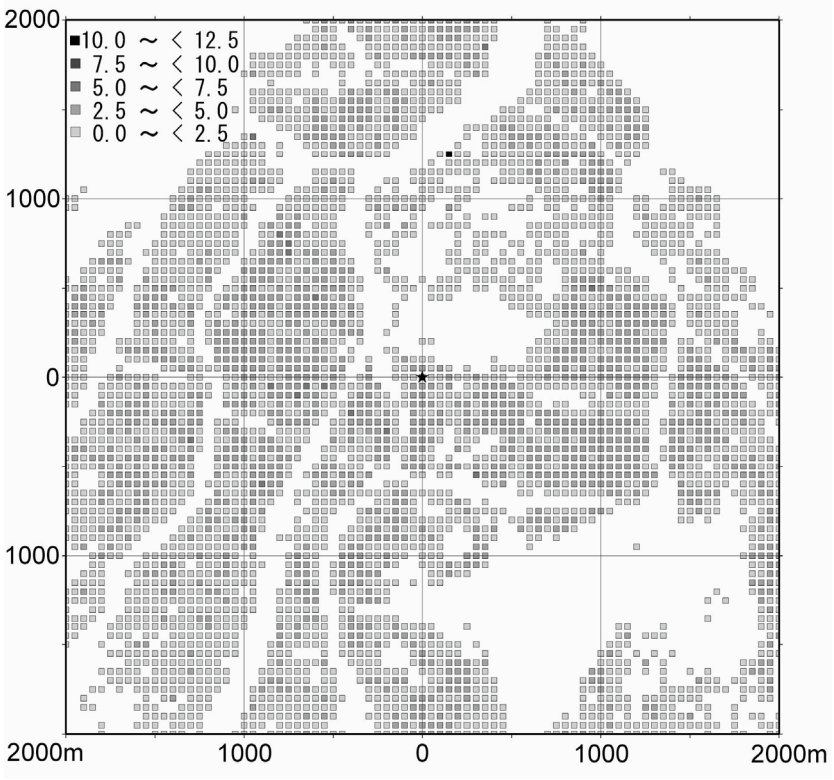

Figure 7 Distribution of average water flux in each 50 m grid within 4km × 4km area of hypocenter of the A-bomb. A star marked at a location (0 m, 0 m) is the hypocenter of A-bomb. Unit: mm h^{-1} m^{-2}

4.3 Black carbon flux

The estimated carbon flux from the fire induced by the A-bomb was calculated based on the total mass of flammable materials in each grid and the production constant of black carbon (Table 1). As discussed in Section 2, heat and water are produced in proportion to the amount of flammable materials, whereas the amount of carbon produced depends upon the oxygen condition during the fire, which is unknown. We assumed that 10% of flammable materials was under reducing conditions; thus, the total amount of black carbon produced and released during the fire was estimated to be 0.02 Tg. Because the carbon produced is proportional to the water produced (Figure 7), we did not provide a map of the distribution of black carbon flux.

5. Conclusions

The average heat flux in the region of the Hiroshima A-bomb hypocenter was 14.4 kJ $s^{-1}m^{-2}$, and it ranged from 0.5 to 96.5 kJ s^{-1} m^{-2}. The total heat released during the fire induced by the explosion was 7 PJ. In total, 0.22 Tg of water was produced and released during the fire. The total amount of black carbon produced and released during the fire was 0.02 Tg when we assume that 10% of fuel was under reducing conditions. Time-dependent fluxes of heat, water, and carbon were also calculated in each 50 m grid. These latest heat, water, carbon dioxide, and black carbon fluxes would be used as boundary conditions for the chemical transport models to obtain more reliable results on local fallout from the Hiroshima A-bomb.

Acknowledgemen

The authors thank Tomoko Kudo, Sachiko Yoshimura, Shoko Shimada, Sachie Ishikawa and Aoi Mori for their work in preparing the database, figures, and tables for this article.

References

DiNenno, Philip J., Craig L. Beyler, Richard L. P. Custer, W. Douglas Walton, John M. Watts, Dougal Drysdale, John R. Hall (Eds.). 1995a. Table 3-4.11: Yields of fire products and chemical, convective, and radiative heats of combustion for well-ventilated fires, 3-78. In: SFPE Handbook of Fire Protection Engineering, 2nd ed. The National Fire Protection Association, Quincy, Massachusetts.

DiNenno, Philip J., Craig L. Beyler, Richard L. P. Custer, W. Douglas Walton, John M. Watts, Dougal Drysdale, John R. Hall (Eds.). 1995b. Table 3-6.11: Examples of gas temperature-time curves of post-flashover compartment fires for different values of the fire load density and the opening factor, 3-144. In: SFPE Handbook of Fire Protection Engineering, 2nd ed. The National Fire Protection Association, Quincy, Massachusetts.

Hiroshima City. 1971. Hiroshima Genbaku Sensaishi Vol.1 (Hiroshima Atomic Bomb Damages). (in Japanese)

Kawano, N., M. Ohtaki, T. Okada. 2011. Visualized map of a fire field near epicenter of Hiroshima A-bomb in August 6, 1945, 15-24. In: M. Aoyama and Y. Oochi (Eds.), Revisit the Hiroshima A-bomb with a Database: Latest Scientific View on Local Fallout and Black Rain, Hiroshima City, Hiroshima.

Koizumi, T. 2011. Digital mapping of urban area of Hiroshima City just before and after the atomic bombing, 25-35. In: M. Aoyama and Y. Oochi (Eds.), Revisit the Hiroshima A-bomb with a Database: Latest Scientific View on Local Fallout and Black Rain, Hiroshima City, Hiroshima.

Okada, Y., M. Aoyama. 2011. Resources of heat, water and carbon fluxes for an induced urban fire in 1945 Hiroshima based on field research of Japanese traditional houses, 37-41. In: M. Aoyama and Y.

Oochi (Eds.), Revisit the Hiroshima A-bomb with a Database: Latest Scientific View on Local Fallout and Black Rain, Hiroshima City, Hiroshima.

Petterson, R.C., 1984. The chemical composition of wood, 7-126. In: Wowell, R. M. (Ed) “The Chemistry of SolidWood”. Advances in Chemistry Series 207. American chemical society. Washington, D.C.